Massachusetts Institute of Technology
Artificial Intelligence Laboratory
and
Center for Biological Information Processing

A.I. Memo 849
C.B.I.P. Paper 013

June, 1985

CHARACTERIZATION OF JOINT-INTERPOLATED ARM MOVEMENTS

John M.Hollerbach and Christopher G. Atkeson

Abstract: Two possible sets of planning variables for human arm movement are joint angles and hand position. Although one might expect these possibilities to be mutually exclusive, recently an apparently contradictory set of data has appeared that indicates straight-line trajectories in both hand space and joint space at the same time. To assist in distinguishing between these viewpoints applied to the same data, we have theoretically characterized the set of trajectories derivable from a joint based planning strategy and have compared them to experimental measurements. We conclude that the apparent straight lines in joint space happen to be artifacts of movement kinematics near the workspace boundary.

This paper describes research done at the Department of Psychology and at the Artificial Intelligence Laboratory of the Massachusetts Institute of Technology. Support for this research was provided by NIH Research Grant AM 26710, awarded by the National Institute of Arthritis, Metabolism, and Digestive Diseases, and by an NSF Graduate Fellowship (CGA). The support for the facilities at the Artificial Intelligence Laboratory is provided in part by the Defense Advanced Research Projects Agency under Office of Naval Research contract N00014-80-C-0505.

1 Introduction

In considering how the motor control system executes an arm trajectory from a starting point to a goal point, one hypothesis is that a detailed time sequence of arm positions is planned along the trajectory. The two most obvious candidates for the planning variables that specify arm position are (1) joint angles and (2) hand position and orientation. To decide between these possibilities, researchers have sought the variables that give the most parsimonious description of experimental arm trajectories. Morasso (1981) observed that arm movements restricted to a horizontal plane were approximately straight, a finding corroborated by other researchers (Abend, Bizzi, and Morasso 1982; Hollerbach and Flash, 1982). Since the joint angle trajectories are apparently complicated functions of the start and goal points, Morasso argued that the manifest simplicity of the hand variable description can be considered as evidence for planning in hand variable space (Fig. 1).

Other researchers have reported evidence for joint space planning. Kots and Syrovegin (1966) found a constant ratio of angular speed for simultaneous movements in elbow and wrist, although these findings have been criticized by Bishop and Harrison (1977). The most intriguing evidence, which triggered the investigations of this paper, is provided in a series of papers on two-joint arm movements in a vertical plane (Soechting and Lacquaniti, 1981; Lacquaniti and Soechting, 1982; Lacquaniti, Soechting, and Terzuolo, 1982; Soechting and Lacquaniti, 1983). To quote the earliest paper:

> "The other consistent findings which characterize the pointing movement examined can be summarized as follows: (1) the ratio of the maximal velocity of the elbow to that at the shoulder is equal to the ratio of the angular excursion at the two joints, (2) the two angular velocities reach a maximum at the same time and (3) their slope is independent of target location as the target is approached. These invariances are all expressed in intrinsic coordinates and, thus, one may pose the question: Is the movement organized in terms of its intrinsic coordinates (θ [shoulder angle] and ϕ [elbow angle]) rather than in terms of extrinsic coordinates (x, y)?"[1]

The reason this evidence is intriguing is that at the same time the joint rate ratios seem constant, inspection of the trajectories shows approximately straight-line hand

[1] Soechting and Lacquaniti (1981), p. 718.

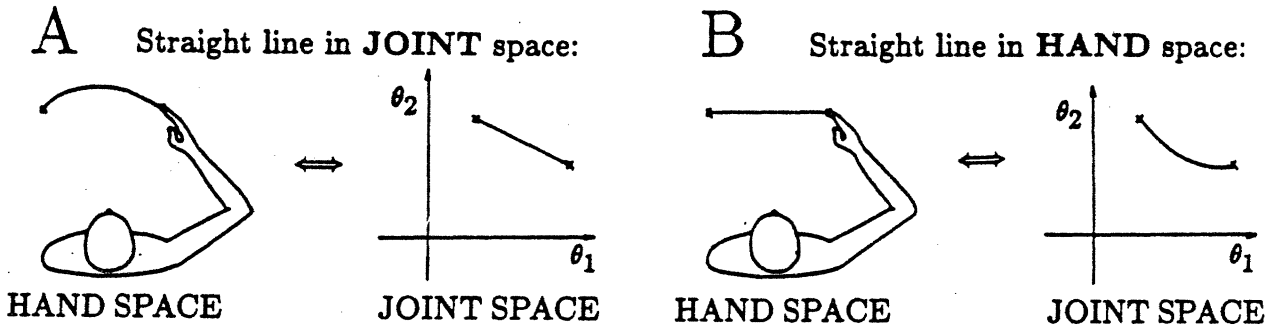

Figure 1: **A:** A diagram of a straight line movement in joint space and the corresponding path in hand space. **B:** A straight-line movement in hand space and the corresponding path in joint space. (θ_1 is the shoulder angle and θ_2 is the elbow angle.)

paths (Fig. 4). It would be expected that these two viewpoints exclude each other, given the complex transformation between joint space and hand space. There are only two degrees of freedom in a two-joint arm and either a hand trajectory or a joint trajectory completely specifies the motion of the arm.

In this paper we reconcile this discrepancy by showing that the joint rate ratio plots are not actually constant despite their appearance. The two viewpoints are generally exclusive and clearly distinguishable, as we show by a theoretical characterization of all possible straight-line joint paths. To explain why the data seem to support both viewpoints, we will focus on the property for the corresponding experimental movements of unidirectional execution towards the workspace boundary. It will be shown that a general kinematic property of two-link mechanisms at the boundary of the workspace is the approach of the joint rate ratios to a constant value. Thus it is unnecessary to invoke motor system planning and control to explain the joint space characteristics.

2 Results

In this section we derive a succinct mathematical formulation for the set of all possible trajectories obtainable from a strategy of constant joint rate ratio. This formulation allows determination of the extent to which these trajectories are distinguishable from hand-based straight-line trajectories. Next, a surprising kinematic behavior of a two-

link mechanism as it approaches the workspace boundary is presented, and is invoked to explain the apparent contradiction of straight-line paths simultaneously in hand and joint space.

2.1 Joint Interpolation

In the introduction we contrasted straight-line motions in hand space to straight-line motions in joint space. We will first show that a strategy of maintaining a constant joint rate ratio is equivalent to executing straight lines in joint angle space. In robotics straight lines in joint space are known as joint interpolation (Brady, 1982), defined by the following equation (see Fig. 1a):

$$\boldsymbol{\theta}(t) = \Big(\boldsymbol{\theta}(t_f) - \boldsymbol{\theta}(t_i)\Big) f(t) + \boldsymbol{\theta}(t_i)$$

where $\boldsymbol{\theta} = (\theta_1, \theta_2, \ldots, \theta_n)$ is a vector of the n joint angles, $\boldsymbol{\theta}(t_i)$ are the joint angles at the start of the movement, $\boldsymbol{\theta}(t_f)$ are the joint angles at the end of the movement, and $f(t)$ is any monotonic time function ($\dot{f}(t) \geq 0$) with $f(t_i) = 0$, $f(t_f) = 1$. Note that each joint angle will have the same velocity profile except for a scaling factor of distance travelled by that joint. In these trajectories all joints reach maximal velocity at the same time and the ratio of any pair of maximal velocities equals the corresponding ratio of angular excursions of the joints.

To begin the demonstration of equivalence, the ratio of any two joint-angular velocities given a joint interpolation strategy is:

$$\frac{\dot{\theta}_j(t)}{\dot{\theta}_k(t)} = \frac{\Big(\theta_j(t_f) - \theta_j(t_i)\Big)\dot{f}(t)}{\Big(\theta_k(t_f) - \theta_k(t_i)\Big)\dot{f}(t)} = \frac{\Delta\theta_j}{\Delta\theta_k}$$

which is constant. On the other hand, a constant joint rate ratio strategy implies a constant slope of the trajectory in joint angle space, since by the chain rule:

$$\frac{\dot{\theta}_2}{\dot{\theta}_1} = \frac{d\theta_2}{dt}\frac{dt}{d\theta_1} = \frac{d\theta_2}{d\theta_1}$$

which is constant (Fig. 2a). Straight lines are not the only possible planning strategy in terms of joint variables, but they are the most common and the most analyzed. Other

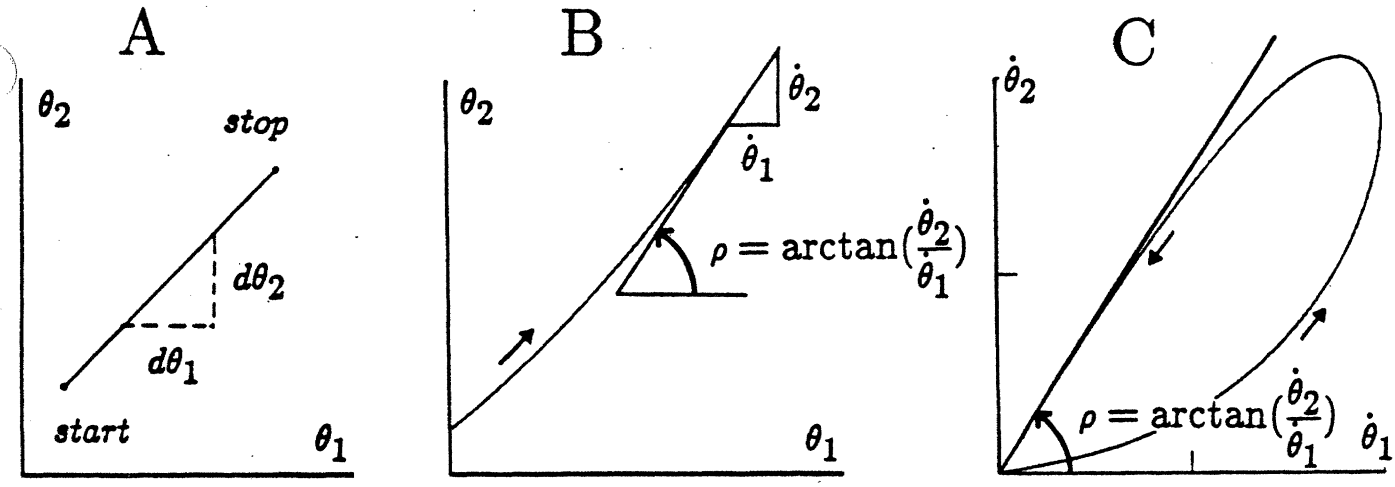

Figure 2: **A:** A constant slope in joint space (which leads to a straight line) implies a constant joint rate ratio and vice versa. The slope of the line in joint space is $\dot{\theta}_2/\dot{\theta}_1$. **B:** Segments of the joint space path (in this case a segment of trajectory 1 from figure 5) can be fit by straight lines whose slope is given by $\dot{\theta}_2/\dot{\theta}_1$ and whose angle from the vertical is given by $\rho = \arctan(\dot{\theta}_2/\dot{\theta}_1)$. **C:** The same result can be seen in the joint velocity space trajectory where the path approaches a straight line asymptote towards the end of the movement whose slope is $\dot{\theta}_2/\dot{\theta}_1$ and whose angle from the origin is $\rho = \arctan(\dot{\theta}_2/\dot{\theta}_1)$. We use the angle ρ to describe the joint rate ratio since the arctangent of a ratio remains between $-\pi$ and π as the ratio itself can vary between negative and positive infinity.

conceivable strategies include independent joint control, where each joint has a separate time function.

The implication of this analysis is that the features of trajectories that can be used to support joint variable planning are straight-line segments in joint angle space. Soechting and Lacquaniti (1981) actually presented more complicated trajectories for which only a portion of the joint angle plots, in the deceleratory phase, seemed a straight line. Local straight segments of a path can be inferred either by examination of the joint angle plots (Fig. 2b) or by the asymptotic approach in joint velocity space (Fig. 2c). A goal in the subsequent sections is to understand when such straight line segments in joint angle space arise.

2.2 The N-Leaved Rose

One possible problem is that the trajectories produced by a joint interpolation strategy may be experimentally indistinguishable from trajectories produced by a hand space strategy. To test for this possibility we have theoretically characterized what paths straight-line movements in joint space will produce in hand space for a planar two-link arm (Fig. 3a). This two-link arm is a reasonable approximation to the forearm and upper arm of a human, since the experimental data typically describes planar movements involving only the shoulder and elbow joints. The features of all straight-line joint space motions of this two-link arm can be described rather simply. For a constant joint rate ratio $K = \dot{\theta}_1/\dot{\theta}_2$ and an initial arm position at full extension ($\theta_1 = 0$, $\theta_2 = 0$), we generate a straight line in joint space and a more complex curve in hand space. This can be done for any joint rate ratio, to generate a family of corresponding curves in joint space (Fig. 3b) and in hand space (Fig. 3c). All features of joint interpolated paths have been generated, due to the rotational symmetry of this arrangement with respect to θ_1, in that a shift in the initial condition $\theta_1(0)$ merely shifts Fig. 3b to the left or the right and rotates Fig. 3c about the origin by $\theta_1(0)$ without changing path shape.

It is possible to characterize analytically the family of curves generated by joint-interpolated trajectories in a succint form by using a polar coordinate (r, ϕ) arm description (Fig. 3a), with r the radial distance from the shoulder to the arm tip and ϕ the angle the radial line makes at the shoulder:

$$\phi = \theta_1 + \frac{\theta_2}{2}, \qquad r = 2\cos\frac{\theta_2}{2},$$

$$\dot{\phi} = \dot{\theta}_1 + \frac{\dot{\theta}_2}{2}, \qquad \dot{r} = -\dot{\theta}_2 \sin\frac{\theta_2}{2}.$$

Combining equations,

$$\dot{\phi} = \left(\frac{\dot{\theta}_1 + \dot{\theta}_2/2}{\dot{\theta}_2}\right) \frac{-\dot{r}}{\sin(\theta_2/2)}.$$

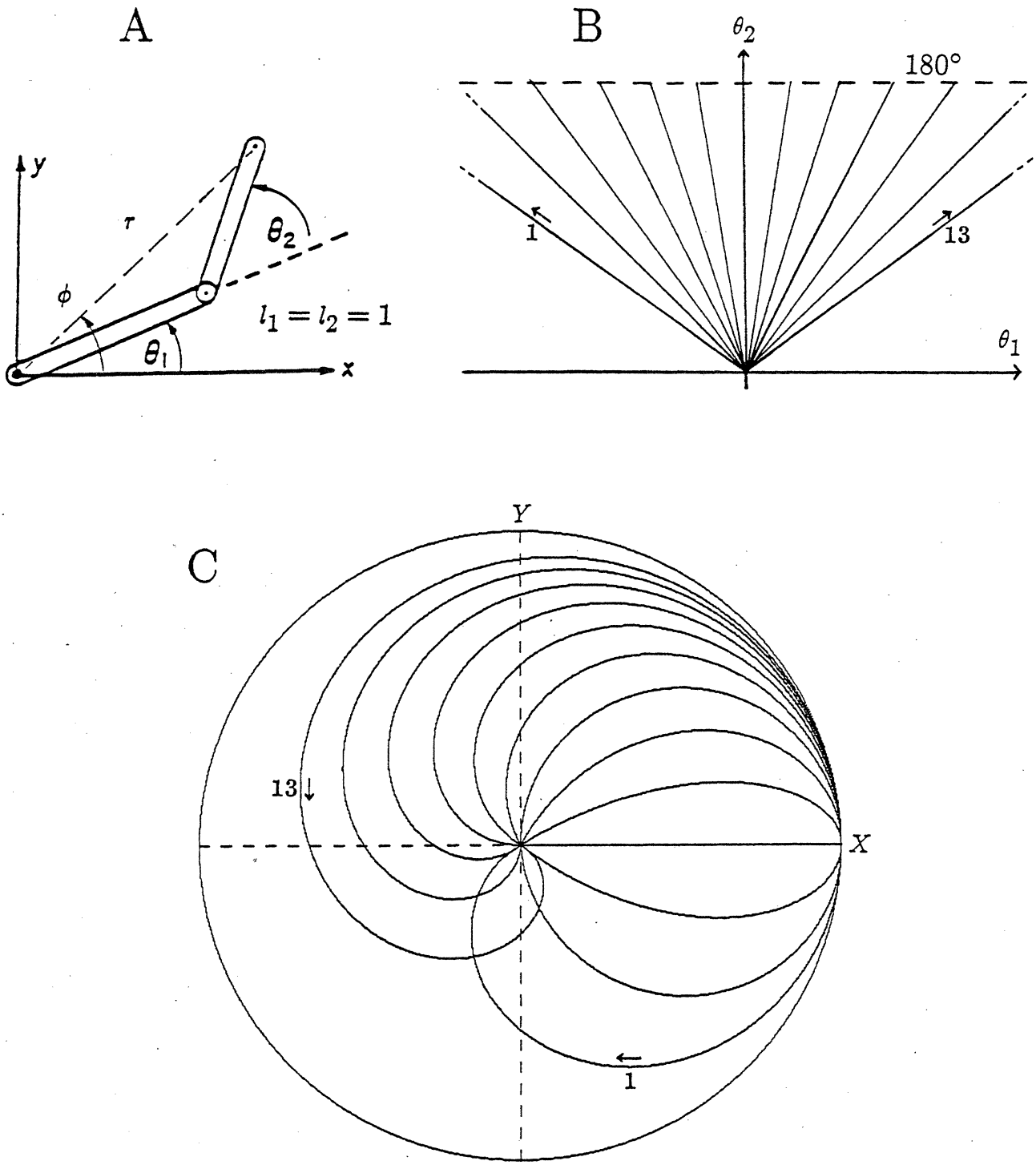

Figure 3: **A:** A planar two link arm. (θ_1, θ_2) are the joint angles and (r, ϕ) is the polar coordinate description of the tip position (x, y). For this figure we took the link lengths, $l1$ and $l2$, to be equal to 1. **B:** A sampling of the straight lines in joint space from the origin. Note that the origin in joint space corresponds to a fully extended arm whose tip is at $x = 2$, $y = 0$. **C:** The straight line joint space trajectories of B mapped to hand space.

Suppose $K = \dot{\theta}_1/\dot{\theta}_2$ is constant. Then

$$\dot{\phi} = (K + 1/2)\frac{-\dot{r}}{\sin(\theta_2/2)}.$$

Noting that $\sin(\theta_2/2) = \sqrt{1 - (r/2)^2}$ and integrating the equation

$$\int_0^t \dot{\phi}\, dt = \int_0^t \frac{-\dot{r}}{\sqrt{1 - (r/2)^2}}\, dt$$

yields

$$\phi - \phi_0 = (2K + 1)\left(\cos^{-1}(\frac{r}{2}) - \cos^{-1}(\frac{r_0}{2})\right).$$

Taking $\cos^{-1}(r_0/2) = 0$, where the arm is initially fully extended, we obtain the

N-LEAVED ROSE: $\boxed{r = 2\cos\left(\frac{\phi - \phi_0}{2K + 1}\right)}$

As can be seen in Fig. 3c, N-leaved roses (Burlington, 1942) tend to be strongly curved, especially for movements that are not primarily radial movements. Hence joint-based planning generally yields trajectories readily distinguishable from straight-line hand paths. There is exactly one special case in which straight-line paths exist simultaneously in hand space and in joint space, when $\dot{\theta}_1 = -\dot{\theta}_2/2$ and hence $\dot{\phi} = 0$. The trajectory must then follow a straight radial line through the shoulder. The horizontal straight line in Fig. 3c is an example, and corresponds to a degenerate "rose petal" with no width. In examining the movements of Figs. 4a and 5a, it seems movement 6 does fall into this special category and movement 5 nearly does, but movements 1-4 cannot be explained in this way.

2.3 Movements Towards The Workspace Edge

2.3.1 Simulated Movements

Though the previous analysis has shown that in general joint-interpolated movements are strongly curved, it nevertheless remains to explain why the data of Soechting and

Lacquaniti (1981) apparently show approximately straight-line hand paths and, during the last half of the trajectories, an approach to a constant joint rate ratio (Fig. 4).

One possibility is that the small deviations from hand-space straight lines seen in the data are significant and explain the constant joint rate ratio asymptote. To decide on this possibility, we simulated exactly straight-line movements with approximately the same starting and target points as in a sample of the original data (Fig. 4a). For these simulated movements we used link lengths measured from a human subject and the trajectories were minimum jerk (Hogan 1984). The simulated straight-line movement paths are shown in Fig. 5a and the corresponding joint-space trajectories are shown in Fig. 5b.[2] We note that the second half of each of these joint-space trajectories approaches a straight line in both the real and simulated data, which apparently suggests that the last half of the movement is joint interpolated. The joint velocity-space diagrams show the same features in the real and simulated data: an approach to an asymptote and the transition from an oval trajectory to a narrower trajectory as the final target shifted (Figs. 4c-i and 5c).

To pursue further the issue of a constant joint rate ratio, the plot of $\arctan(-\dot{\theta}_2/\dot{\theta}_1)$ versus normalized movement distance (the distance traveled so far divided by the total distance) in Fig. 5d evidently shows the approach of the joint rate ratios to a constant. There is clearly something special about these movements that goes against the expectations based on N-leaved roses, and the following section explores why this is the case.

2.3.2 Kinematic Constraints

When the straight lines of Fig. 5a are extended to the workspace boundary, it can be seen that the plots of Fig. 5d actually reach the same constant limit in Fig. 6a. To explain this result, we examine the behavior of the analytic expression for joint rate ratio as the boundary is approached. The general analytic expression is (see Appendix for derivation):

[2] We have used standard coordinate systems and joint angle conventions from robotics. This leads to apparent differences between figures 4 and 5 in terms of scales and orientation of the plots. We have tried to minimize these apparent differences by rearranging the units of the various axis.

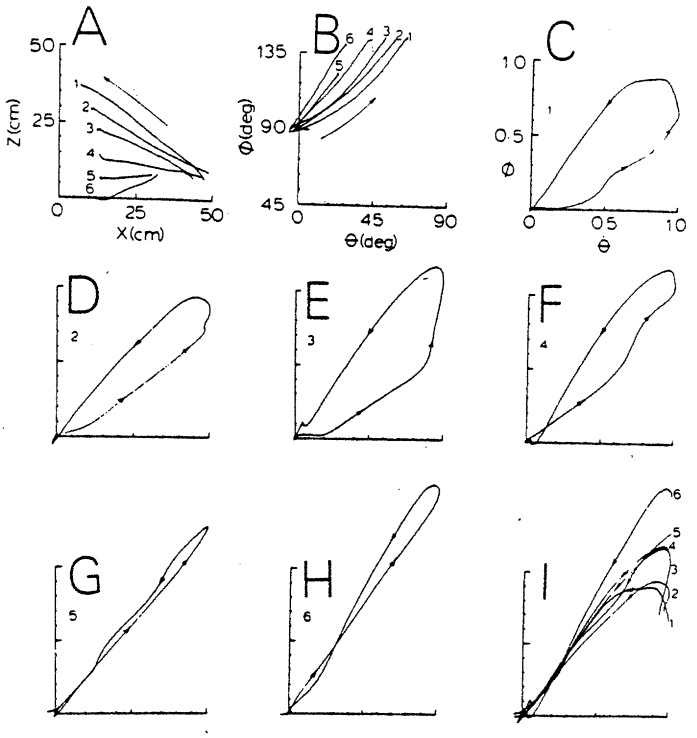

Figure 4: [Figure 4 and accompanying legend from figure 4 of (Soechting and Lacquaniti, 1981)] "Dependence of movement trajectory on target location. **A:** Movement trajectories of individual trials to six target locations described in x, z coordinates; **B:** The same movements described in θ, ϕ coordinates. Lower target locations require progressively less shoulder flexion. **C** to **H:** The trajectories described in the phase plane $(\dot{\theta}, \dot{\phi})$ for movements to targets 1 to 6, respectively. Only the portions beginning when shoulder angular velocity is maximal is shown in **I**. Note that the trajectories form a loop which becomes progressively tighter for lower target locations and that the terminal portions of all trajectories are virtually superimposable." [(Soechting and Lacquaniti, 1981) use different joint angles; θ is the shoulder angle: $(\theta = \theta_1 + 90°)$, and ϕ is the elbow angle: $(\phi = 180° - \theta_2)$]

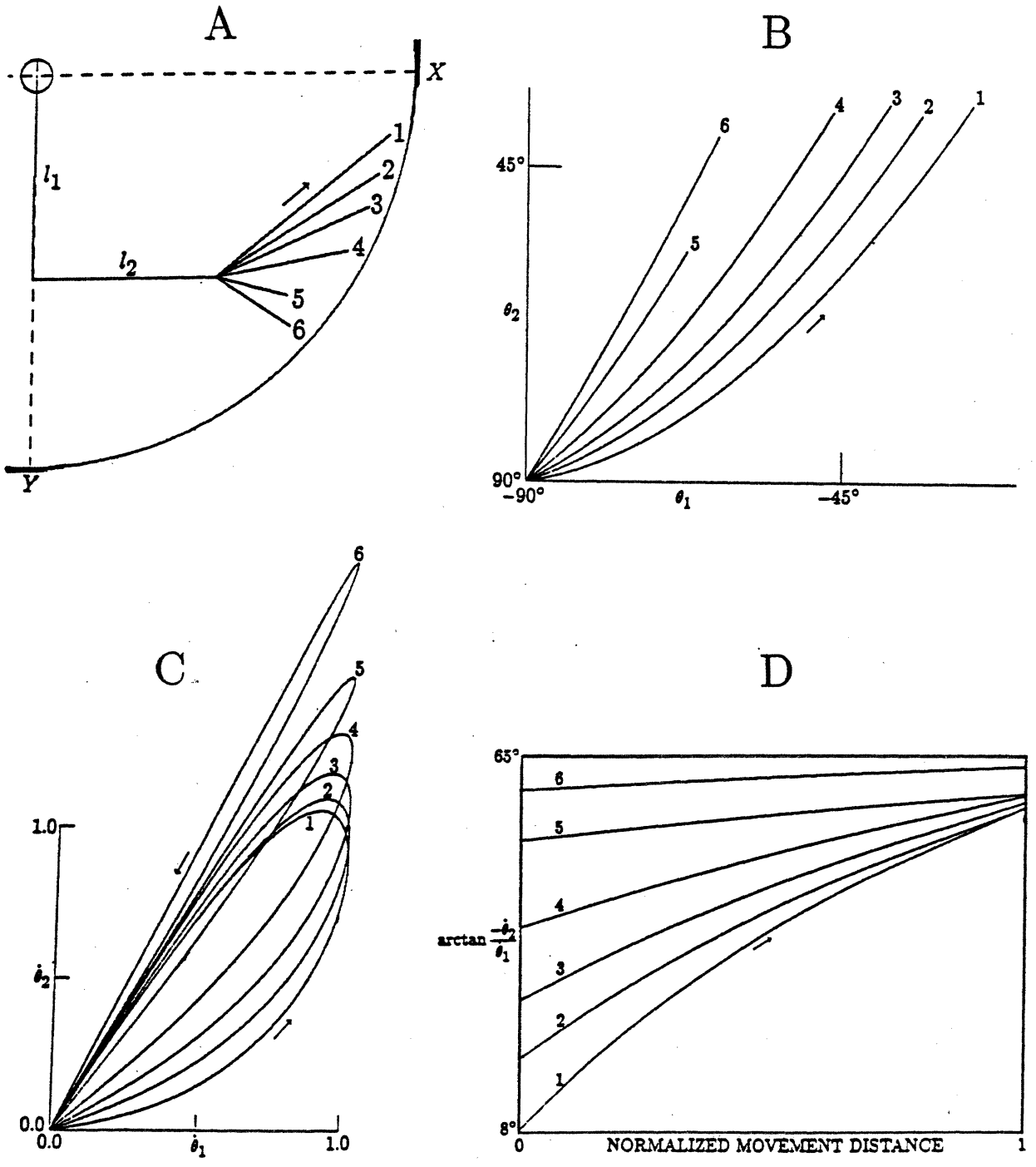

Figure 5: **A:** Six simulated straight-line hand space movements. The start and target points for these six movements correspond to those for the six movements of (Fig. 4A). The movements are displaced and reversed in direction only due to different coordinate system conventions. **B:** The corresponding paths in joint space. These paths should match the joint-space paths of (Fig. 4B). (We use different joint angle conventions from Fig. 4: $\theta = \theta_1 + 90°$, $\phi = 180° - \theta_2$). **C:** The normalized joint velocity-space trajectories. These trajectories should match those in Figs. 4C to 4I. **D:** The actual joint rate ratios (in angular form) for each movement plotted as the $\arctan(-\dot{\theta}_2/\dot{\theta}_1)$ of the points in velocity space versus normalized movement distance. The joint rate ratios all seem to approach a limit, even for these exactly straight-line movements in hand space.

$$\text{Joint rate ratio} = \frac{\text{elbow angular velocity}}{\text{shoulder angular velocity}} = \frac{\dot{\theta}_2}{\dot{\theta}_1}$$
$$= \frac{-\dot{x}l_1 \cos\theta_1 - \dot{y}l_1 \sin\theta_1 - \dot{x}l_2 \cos(\theta_1+\theta_2) - \dot{y}l_2 \sin(\theta_1+\theta_2)}{\dot{x}l_2 \cos(\theta_1+\theta_2) + \dot{y}l_2 \sin(\theta_1+\theta_2)}.$$

Near the periphery, the elbow becomes straight and $\theta_2 \to 0$.

$$\lim_{\theta_2 \to 0} (\text{joint rate ratio}) = \lim_{\theta_2 \to 0} \frac{\dot{\theta}_2}{\dot{\theta}_1} = -\frac{l_1 + l_2}{l_2}$$

Surprisingly, the joint rate ratio is a constant, dependent only on the link lengths. The constancy holds for any point on the workspace boundary and for any trajectory that approaches the boundary. Before the workspace boundary, the joint rate ratios are not constant despite appearances. It is critical to distinguish the statements "is a constant" versus "tending towards a constant." The trajectories of Soechting and Lacquaniti (1981) therefore do not actually demonstrate a constant joint rate ratio in the deceleratory phase, and there is no contradiction with the trajectory features of hand-space straight-line paths.

To show that this is a general kinematic phenomenon for two-link planar mechanisms, we plot a contour map of constant $\arctan(-\dot{\theta}_2/\dot{\theta}_1)$ lines connecting the shoulder point to the movement starting point (Fig. 6b). Overlayed onto this contour map are the extended straight-line hand-space movements of Fig. 5a. As these movements traverse towards the boundary, each crosses the contour lines in a particular order before finally reaching the boundary value of 65°. The experimental movements of Fig. 4a reached at least the 57° contour.

3 Discussion

The misleading constancy of joint rate ratio in the data of Soechting and Lacquaniti (1981) is due to an unfortunate choice of experimental movements. If they had chosen movements in the reverse direction, from the boundary to their original interior starting point, then they would have observed an apparent constancy of joint rate ratio in the

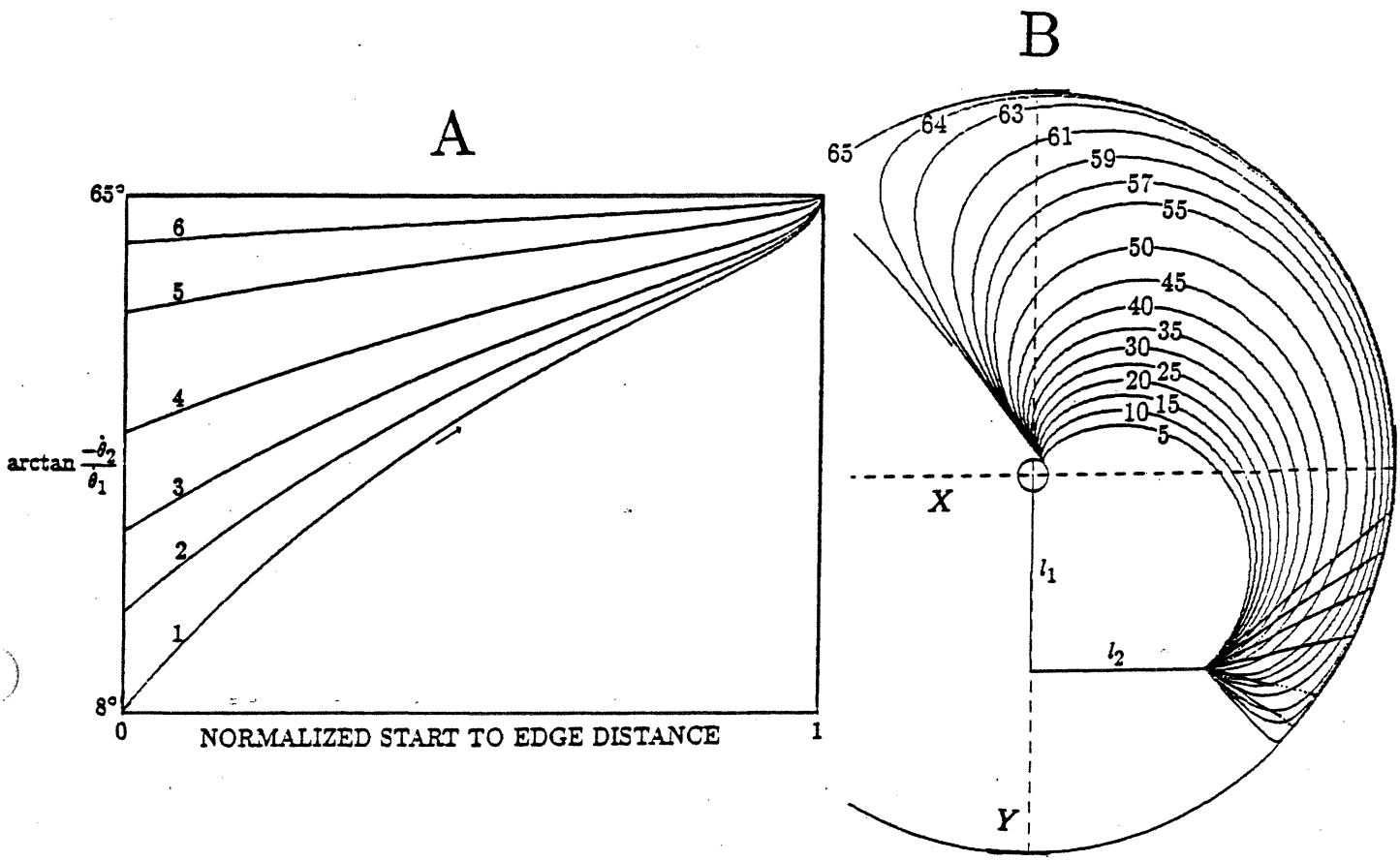

Figure 6: Effect of joint rate ratio limit at edge of workspace. **A:** When the joint rate ratio plots for the simulated movements of figure 5 are plotted all the way to the edge of the workspace the joint rate ratios all reach the same limit. **B:** A contour map can be drawn for the joint rate ratios (in terms of $\arctan(-\dot{\theta}_2/\dot{\theta}_1)$) reached for all straight line hand space trajectories starting at $\theta_1 = -90°$, $\theta_2 = 90°$. Note that the limit of 65° is approached closely in a large portion of the workspace. The simulated movements of figure 5 extended to the edge of the workspace are also shown.

acceleratory rather than deceleratory phase of movement. If they had chosen start and goal points completely interior to the boundary, then they might have observed straight-line hand paths corresponding to complicated functions of joint rate ratio.

While our conclusion is that this experimental data is consistent with straight-line hand paths rather than with straight-line joint paths, we do not wish to imply that humans select only hand-space trajectory plans. What our analysis shows is that if one is interested in the question of joint-space versus hand-space planning, then one should stay away from the workspace boundary. Movements near the boundary will always appear to have a constant joint rate ratio, and there is not a clear enough distinction from hand-path trajectories.

3.1 Explicit vs. Implicit Trajectories

The point-by-point evolution of an arm trajectory need not be the result of an explicit trajectory plan, as would be hypothesized for planning in joint or hand space. An alternative viewpoint is that trajectory shape is an implicit function of control. One example is endpoint control, where the muscle actuation is proportional to error between a current arm state and the end state; the trajectory evolves implicitly through the interaction of movement dynamics and the endpoint-dependent actuation. Hollerbach (1982) proposed a coupled oscillator theory of handwriting in which an individual writing stroke is generally shaped by parameters of the oscillation but is not directly specified. The various proposals for final position control are a form of endpoint control where muscle ensemble equilibrium point is changed in a step-like fashion from start to goal; the muscle properties with or without proprioceptive feedback loops set up force fields that mechanically direct a movement toward an equilibrium goal (Crossman and Goodeve, 1963; Fel'dman, 1974; Bizzi, Polit, and Morasso, 1976; Kelso, 1977; Kelso and Holt, 1980).

Evidence has been accumulating against endpoint control and for intermediate trajectory points. Delatizky (1982) concluded from simulation that it is unlikely such a simple mechanism could generate observed straight-line hand paths with bell-shaped velocity profiles. Bizzi et al. (1982) inferred the existence of intermediate trajectory

points through perturbation experiments. An alternative hypothesis is that trajectory generation is the outcome of some continuous process or internal (mental) dynamic system, as described in (Saltzman and Kelso, 1983).

Explicit trajectory planning has still not been conclusively demonstrated, but there are reasons for hypothesizing its existence. Planning in hand space allows handling external task constraints such as motion along geometric constraint surfaces (Hollerbach, 1982), obstacle avoidance (Lozano-Perez, 1982), and minimization of load perturbation (Flash, 1982). The cost of hand space planning is that it requires transformations between hand position variables and the directly sensed and controlled variables such as joint angles and muscle lengths. Simple paths in hand space such as straight lines can lead to complex trajectories in joint space (Fig. 1b).

The advantage of planning in joint space is that it simplifies the planning process. Each joint has an initial angle and a final angle, and a smooth transition is simply generated from the initial to the final angle for each joint individually. Coordinating the joints need only be done by coordinating the timing for joint motion start and stop. A simple joint plan such as this will lead to straight line paths in joint space if the movements of each joint are amplitude scaled versions of each other. The problem with this form of arm motion planning is that it often generates complex trajectories of the hand (Fig. 1a), which may cause collision with obstacles or unwanted forces on a hand-held load.

The question of what spaces or sets of coordinates are used in the planning and control of human movement cannot be settled on the basis of kinematic data alone, given that the kinematic data is in general complex and the shapes of movements can reflect a wide variety of task demands. However, discovering simple models that explain a wide variety of kinematic behavior give strong indications of what types of signals and processes exist in human motor control. Since the simple description of point-to-point trajectories as handspace straight line motions seems to apply throughout the workspace we take this as evidence of trajectory planning at a level higher than muscle or joint variables.

3.2 Summary

- A strategy of constant joint rate ratio of shoulder and elbow joints is formally equivalent to joint interpolation, i.e., straight line paths in joint space.

- For a given joint rate ratio, all hand trajectory points lie on a polar coordinate curve called an N-leaved rose whose locus is independent of the exact time profile. These N-leaved roses tend to be strongly curved, so that joint based planning generally yields trajectories readily distinguishable from straight line hand paths.

- However, in movements towards the edge of the workspace the ratio of shoulder angular velocity and elbow angular velocity tends towards a constant value no matter how the edge of the workspace is approached. This is a general property of two-link mechanisms, arising solely from kinematics.

- We note that the experimental movements provided as evidence for joint based planning were unidirectional towards the boundary of the workspace. In this situation even a straight line path in hand space approaches a constant joint rate ratio. Thus it is inappropriate to suggest a planning strategy in terms of joint angles on the basis of this evidence, which is an artifact of arm kinematics.

- All the data presented so far is consistent with and can be most concisely explained by planning straight line movements in hand space.

Appendix

In this appendix we derive an analytic expression for the joint rate ratio given the tip velocity for a simple 2 joint arm (Figure 3A). The direct kinematics are

$$x = l_1 \cos(\theta_1) + l_2 \cos(\theta_1 + \theta_2)$$

$$y = l_1 \sin(\theta_1) + l_2 \sin(\theta_1 + \theta_2)$$

where (x, y) is the tip position, θ_1 and θ_2 are the joint angles, and l_1 and l_2 are the link lengths. In order to find the joint velocities we differentiate the above equations:

$$\begin{bmatrix} \dot{x} \\ \dot{y} \end{bmatrix} = \begin{bmatrix} -l_1 \sin(\theta_1) - l_2 \sin(\theta_1 - \theta_2) & -l_2 \sin(\theta_1 + \theta_2) \\ l_1 \cos(\theta_1) + l_2 \cos(\theta_1 + \theta_2) & l_2 \cos(\theta_1 + \theta_2) \end{bmatrix} \begin{bmatrix} \dot{\theta}_1 \\ \dot{\theta}_2 \end{bmatrix}$$

where the 2×2 matrix relating these two vectors is the *Jacobian* $\mathbf{J}$. The joint rate ratio can be found by inverting $\mathbf{J}$.

$$\begin{bmatrix} \dot{\theta}_1 \\ \dot{\theta}_2 \end{bmatrix} = \frac{\begin{bmatrix} l_2 \cos(\theta_1 + \theta_2) & l_2 \sin(\theta_1 + \theta_2) \\ -l_1 \cos(\theta_1) - l_2 \cos(\theta_1 + \theta_2) & -l_1 \sin(\theta_1) - l_2 \sin(\theta_1 + \theta_2) \end{bmatrix}}{\text{determinant}(\mathbf{J})} \begin{bmatrix} \dot{x} \\ \dot{y} \end{bmatrix}$$

and therefore

$$\begin{aligned} \text{Joint rate ratio} &= \frac{\text{elbow angular velocity}}{\text{shoulder angular velocity}} = \frac{\dot{\theta}_2}{\dot{\theta}_1} \\ &= \frac{-\dot{x} l_1 \cos\theta_1 - \dot{y} l_1 \sin\theta_1 - \dot{x} l_2 \cos(\theta_1 + \theta_2) - \dot{y} l_2 \sin(\theta_1 + \theta_2)}{\dot{x} l_2 \cos(\theta_1 + \theta_2) + \dot{y} l_2 \sin(\theta_1 + \theta_2)} . \end{aligned}$$

4 References

ABEND, W., BIZZI, E. AND MORASSO, P. (1982) Human arm trajectory formation. Brain 105:331-348

BISHOP, A. AND HARRISON, A. (1977) Kots and Syrovegin (1966) - a demonstration of modular units in motor programming?. J Human Movement Studies 3:99-109

BIZZI, E., ACCORNERO, N., CHAPPLE, W., AND HOGAN, N. (1982) Arm trajectory formation in monkeys. Exp Brain Res 46:139-143

BIZZI, E., ACCORNERO, N., CHAPPLE, W., AND HOGAN, N. (1984) Posture control and trajectory formation during arm movement. J Neurosci 4:2738-2745

BIZZI, E., POLIT, A. AND MORASSO, P. (1976) Mechanisms underlying achievement of final head position. J Neurophysiol 39:435-444

BRADY, J.M. (1982) Trajectory planning. In: Brady, J.M., Hollerbach, J.M., Johnson, T.L., Lozano-Perez, T., and Mason, M.T.(eds) Robot Motion: Planning and Control. Cambridge, MIT Press, pp 221-244

BURLINGTON, R.S. (1942) Handbook of Mathematical Tables and Formulas. Sandusky, Ohio, Handbook Publ Inc, pp 33

CROSSMAN, E.R.F.W. AND GOODEVE, P.J. (1983) Feedback control of hand-movement and Fitts' Law. Paper presented at the meeting of the Experimental Psychological Society, Oxford, July 1963, published in Quarterly J Exp Psych 35A:251-278

DELATIZKY, J. (1982) Final position control in simulated planar arm movements. Soc Neurosci Abstr 8:283

FELDMAN, A.G. (1974) Change of muscle length due to shift of the equilibrium point of the muscle-load system. Biofizika 19:534-538

FLASH, T. (1983) Organizing principles underlying the formation of hand trajectories. PhD Thesis, Harvard/MIT Division of Health Sciences and Technology

HOGAN, N. (1984) An organizing principle for a class of voluntary movements. J Neurosci 4:2745-2754

HOLLERBACH, J.M. (1981) An oscillation theory of handwriting. Biol Cybern 39:139-156

HOLLERBACH, J.M. (1982) Computers, brains, and the control of movement. Trends Neurosci 5(6):189-192

HOLLERBACH, J.M. AND FLASH, T. (1982) Dynamic interactions between limb segments during planar arm movement. Biol Cybern 44:67-77

KELSO, J.A.S. (1977) Motor control mechanisms underlying human movement reproduction. J Exp Psych: Human Perception and Performance 3:529-543

KELSO, J.A.S. AND HOLT, K.G. (1980) Exploring a vibratory systems analysis of human movement production. J Neurophysiology 43:1183-1196

KOTS, Y.M. AND SYROVEGIN, A.V. (1966) Fixed set of variants of interaction of the muscles of two joints used in the execution of simple voluntary movements. Biofizika 11:1061-1066

LACQUANITI, F. AND SOECHTING, J.F. (1982) Coordination of arm and wrist motion during a reaching task. J Neurosci 2:399-408

LACQUANITI, F., SOECHTING, J.F., AND TERZUOLO, C.A. (1982) Some factors pertinent to the organization and control of arm movements. Brain Res 252:394-397

LOZANO-PEREZ, T. (1982) Task planning. In: Brady, J.M., Hollerbach, J.M., Johnson, T.L., Lozano-Perez, T., and Mason, M.T.(eds) Robot Motion: Planning and Con-

trol. Cambridge, MIT Press, pp 473-498

MORASSO, P. (1981) Spatial control of arm movements. Exp Brain Res 42:223-227

SALTZMAN, E. AND KELSO, J.A.S. (1983) Skilled actions: a task dynamic approach, SR-76, Haskins Laboratory Status Report on Speech Research, pp 3-50

SOECHTING, J.F. AND LACQUANITI, F. (1981) Invariant characteristics of a pointing movement in man. J Neurosci 1:710-720

SOECHTING, J.F. AND LACQUANITI, F. (1983) Modification of trajectory of a pointing movement in response to a change in target location. J Neurophysiol 49:548-564